Eur. Phys. J. B **5**, 15–22 (1998)

THE EUROPEAN PHYSICAL JOURNAL B

Spin correlations in the two-dimensional spin-5/2 Heisenberg antiferromagnet Rb_2MnF_4

Y.S. Lee[1], M. Greven[1,a], B.O. Wells[1], R.J. Birgeneau[1,b], and G. Shirane[2]

[1] Department of Physics, Massachusetts Institute of Technology, Cambridge, MA 02139, USA
[2] Department of Physics, Brookhaven National Laboratory, Upton, NY 11973, USA

Received: 3 March 1998 / Received in final form: 4 May 1998 / Accepted: 19 May 1998

Abstract. We report a neutron scattering study of the instantaneous spin correlations in the two-dimensional spin $S = 5/2$ square-lattice Heisenberg antiferromagnet Rb_2MnF_4. The measured correlation lengths are quantitatively described, with no adjustable parameters, by high-temperature series expansion results and by a theory based on the quantum self-consistent harmonic approximation. Conversely, we find that the data, which cover the range from about 1 to 50 lattice constants, are outside of the regime corresponding to renormalized classical behavior of the quantum non-linear σ model. In addition, we observe a crossover from Heisenberg to Ising critical behavior near the Néel temperature; this crossover is well described by a mean-field model with no adjustable parameters.

PACS. 75.10.Jm Quantized spin models – 75.25.+z Spin arrangements in magnetically ordered materials (including neutron and spin-polarized electron studies, synchrotron-source X-ray scattering, etc.) – 75.30.Gw Magnetic anisotropy

1 Introduction

The physics of the two-dimensional square-lattice quantum Heisenberg antiferromagnet (2DSLQHA) continues to receive much attention. In addition to the basic interest in studying the role of quantum fluctuations in this high-symmetry low-dimensional system, experimental and theoretical efforts have heightened with the discovery that the undoped parent compounds of high-T_c superconductors are typically very good realizations of the spin $S = 1/2$ 2DSLQHA. In particular, neutron scattering experiments on the insulating lamellar copper oxides La_2CuO_4 [1] and $Sr_2CuO_2Cl_2$ [2] have elucidated the spin fluctuations of the 2DSLQHA model for the extreme quantum limit of $S = 1/2$. The measured spin-spin correlation lengths of $Sr_2CuO_2Cl_2$ are quantitatively described [2] by quantum Monte-Carlo results based on the square-lattice nearest-neighbor Heisenberg model [3,8], and by a low-temperature theory based on the quantum non-linear σ model developed by Chakravarty, Halperin, and Nelson (CHN) [4]. The remarkable agreement between the experimental data for $S = 1/2$ and the theoretical results of CHN, as extended by Hasenfratz and Niedermayer (HN) [5], was found not to hold for higher spin values, $S > 1/2$. In particular, in the $S = 1$ 2DSLQHA systems K_2NiF_4 [2] and La_2NiO_4 [6], the measured correlation lengths were found to deviate significantly from the CHN-HN prediction. A systematic high-temperature series expansion study [7] showed that the deviations increase progressively with increasing spin values above $S = 1/2$. Recent Monte-Carlo work [8] suggests that the explanation for this discrepancy may simply be that the series expansion and neutron scattering results are not in the asymptotic low-temperature regime for which the CHN-HN prediction is expected to hold.

For the 2DSLQHA, quantum spin fluctuations strongly renormalize the spin-stiffness and spin-wave velocity in the $S = 1/2$ system $Sr_2CuO_2Cl_2$, but there appears to be no fundamental change from classical behavior. For $S = 5/2$, the 2DSLQHA should be even less affected by quantum renormalization and thus should correspond more closely to a classical spin system. Indeed, high-temperature series expansion studies reveal a near-agreement between the correlation lengths of the $S = 5/2$ 2DSLQHA and the $S = 5/2$ ferromagnetic system, for which the ground state is classical [9]. In addition, upon scaling the temperature by $J_{nn}S(S+1)$, series expansion results [7] indicate that the correlation length of the 2DSLQHA rapidly approaches that of the classical $S = \infty$ case as the spin value is increased progressively from $S = 1/2$ to $S = 5/2$. In order to examine further the role of quantum fluctuations in the models, and their dependence on the spin quantum number, one requires more experimental data for the correlation length of systems well described by the 2DSLQHA Hamiltonian with higher spin.

[a] *Present address:* Department of Applied Physics and Stanford Synchrotron Radiation Laboratory, Stanford University, Stanford, CA 94305, USA.
[b] e-mail: `robertjb@mit.edu`

We report an energy-integrating neutron scattering study of the 2D instantaneous spin-spin correlations in the $S = 5/2$ material Rb_2MnF_4. This paper is organized as follows: Section 2 contains preliminary details about the Rb_2MnF_4 system and about our measurements; Section 3 contains our experimental results and data analysis; in Section 4, we present a comparison with various theories; and Section 5 summarizes our results.

2 Preliminary details

We study a high-quality single crystal of Rb_2MnF_4, which is, in fact, the same as that used in previous neutron studies [10,11]. Rb_2MnF_4 has the K_2NiF_4 crystal structure, space group $I4/mmm$, with square planes of MnF_2 separated by two intervening sheets of non-magnetic ions. The magnetic Mn^{2+} ions ($S = 5/2$) form a square lattice and are antiferromagnetically coupled to their nearest neighbors *via* super-exchange through the intervening F^- ions. The low-temperature in-plane lattice constants are $a = b = 4.20$ Å, and the out-of-plane lattice constant is $c = 13.77$ Å. Over the temperature range of the experiment, 10 K $\leq T \leq$ 110 K, the in-plane lattice constant changes by only $\sim 0.1\%$, so any concomitant temperature variation of the in-plane exchange coupling will have a negligible effect on the spin correlations. The exchange coupling between nearest neighbor spins in adjacent planes is frustrated for this body-centered tetragonal spin structure. As a result, any effective inter-planar coupling is at least six orders of magnitude weaker than the coupling within the planes, leading to the quasi-two-dimensional nature of the spin system. From previous neutron scattering experiments on this and isomorphous materials, it is known that the critical scattering consists of purely two-dimensional spin fluctuations, and no spin-wave dispersion is observable along the **c**-direction, confirming that a 2D spin model is appropriate [12–14].

The physics of the Mn^{2+} square lattice is well described by the simple spin Hamiltonian

$$H = J_{nn} \sum_{\langle i,j \rangle} \mathbf{S}_i \cdot \mathbf{S}_j \; + \; \sum_i g_i \mu_B H_i^A S_i^z, \qquad (1)$$

where the staggered anisotropy field H_i^A represents the effect of the dipolar anisotropy which favors spin alignment along the **c**-axis. From both NMR measurements of the sublattice magnetization [15] and neutron scattering measurements of the spin-wave dispersion [16,17], one obtains $J_{nn} = 7.36 \pm 0.10$ K. The small Ising anisotropy in this predominately Heisenberg Hamiltonian is $\alpha_I = g\mu_B H^A / \sum_{j=nn} J_{nn} S_j \simeq 0.0047$, as deduced from antiferromagnetic resonance and inelastic neutron scattering measurements of the low-temperature spin-wave gap at the magnetic zone center [15,16]. A small three-dimensional (3D) coupling does exist as evidenced by the transition to 3D long-range order which occurs at $T_N = 38.4$ K. Such a 3D coupling usually appears as a coupling between next-nearest-neighbor (*nnn*) planes. However, the weakness of this coupling is evident from magnetic Bragg diffraction, which reveals two domains with different stacking arrangements of ordered MnF_2 planes: one in which *nnn* planes are ferromagnetically aligned and another in which *nnn* planes are antiferromagnetically aligned [10]. This 3D order reflects primarily 2D correlations with Ising critical behavior, since the staggered magnetization of both stacking domains was found to follow the same power law, $M_s = (1 - T/T_N)^{0.16}$ [10]; the observed critical exponent β for the order parameter is much closer to the 2D Ising model value $\beta = 1/8$ than to the conventional 3D values of approximately 1/3.

The experiments were performed on the H4M thermal neutron spectrometer at the Brookhaven High Flux Beam reactor. The Rb_2MnF_4 crystal was aligned with a $(1\bar{1}0)$ axis perpendicular to the scattering plane, thus having the magnetic zone center wave vector $(1/2, 1/2, 0)$ and the **c**-axis in the scattering plane. The spectrometer was operated in the two-axis energy-integrating configuration with collimator sequence 20′-20′-sample-20′. The scattering geometry was chosen so that outgoing neutrons were perpendicular to the MnF_2 planes, thus integrating over energy at constant in-plane momentum transfer $\mathbf{Q}_{2D}$ [13]. In this geometry, the intensity of the detected neutrons is proportional to the static structure factor,

$$S(\mathbf{Q}_{2D}) \simeq \int_{-\infty}^{E_i} S(\mathbf{Q}_{2D}, \omega) d\omega, \qquad (2)$$

where $\mathbf{Q}_{2D}$ is the momentum transfer within the 2D MnF_2 sheets, and ω is the energy transfer. Here, we assume that any variation in the Mn^{2+} form factor has a negligible effect in the integration over ω. Two incident neutron energies, $E_i = 14.7$ meV and $E_i = 41$ meV, were used to verify that the experiment integrates over the relevant dynamic fluctuations properly. Both incident energies are more than an order of magnitude larger than the magnetic energy scale, J_{nn}, in Rb_2MnF_4. By integrating over all energies, we obtain information about the instantaneous (equal-time) spin correlations of the system.

3 Experimental results and analysis

We show in Figures 1 and 2 representative two-axis scans for $E_i = 41$ meV and $E_i = 14.7$ meV, respectively. In order to extract the intrinsic peak widths and amplitudes of the scattering, we fit our data to the form

$$S(q_{2D}) = \sin^2(\phi) \frac{S_\parallel(0)}{1 + q_{2D}^2/\kappa_\parallel^2} + \Big(1 + \cos^2(\phi)\Big) \frac{S_\perp(0)}{1 + q_{2D}^2/\kappa_\perp^2} \qquad (3)$$

convolved with the instrumental resolution function (which is drawn in the top panels of the figures) on top of a sloping background. Here, $\mathbf{q}_{2D} = (Q_x - 1/2,\, Q_y - 1/2,\, 0)$ represents the displacement from the center of the rod of 2D scattering measured in reciprocal lattice units, and ϕ is the angle subtended by $\mathbf{Q}$ and the **c**-axis. The correlation length $\xi_{\parallel,\perp}$ is the inverse of the $\mathbf{Q}$-space width $\kappa_{\parallel,\perp}$. For

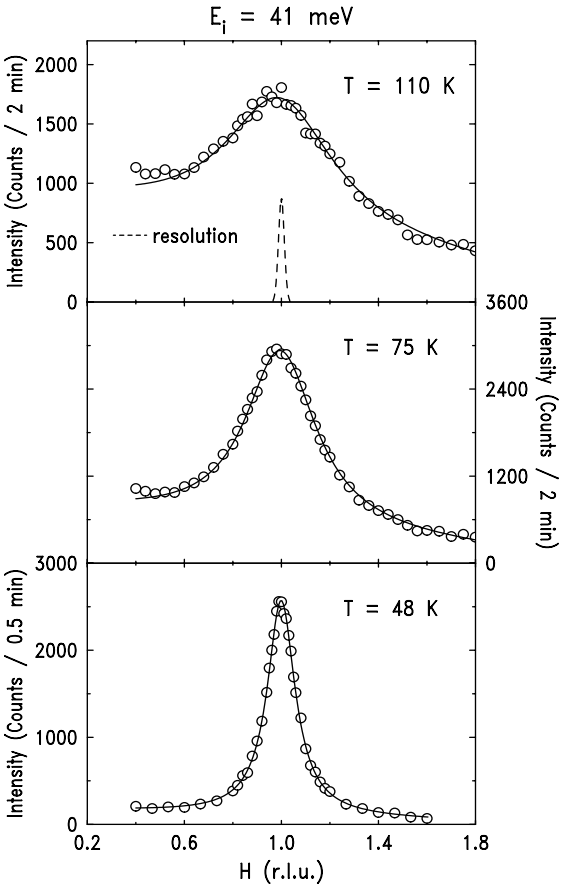

Fig. 1. Representative energy-integrating scans along the direction $(H/2,\ H/2,\ L)$, with L chosen such that $\mathbf{k}_f \parallel \mathbf{c}$, for an incident neutron energy of 41 meV. The solid lines result from least-squares fits of the lineshape, equation (3), convolved with the instrumental resolution. The dashed line in the top panel indicates the instrumental resolution.

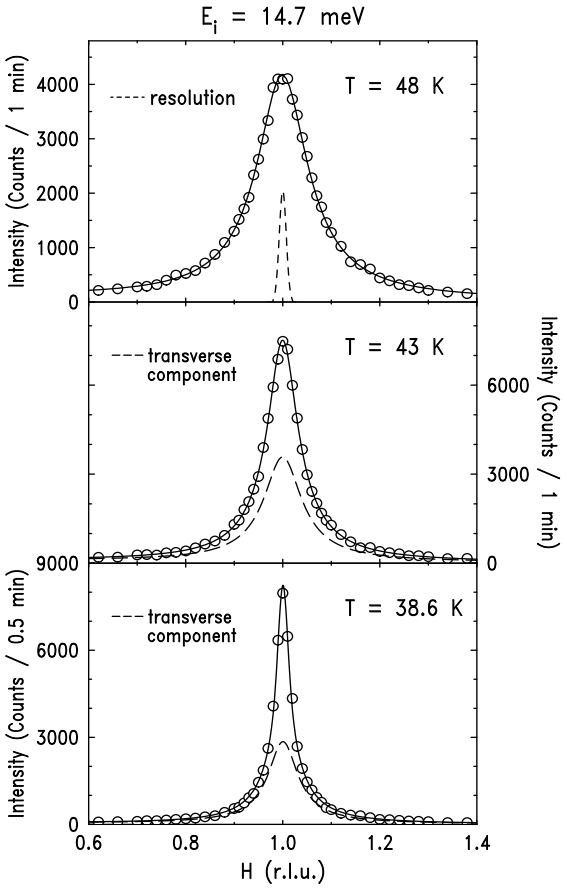

Fig. 2. Representative energy-integrating scans along the direction $(H/2,\ H/2,\ L)$, with L chosen such that $\mathbf{k}_f \parallel \mathbf{c}$, for an incident neutron energy of 14.7 meV. The solid lines result from least-squares fits of the lineshape, equation (3), convolved with the instrumental resolution. The dashed line in the top panel indicates the instrumental resolution. The dashed lines in the bottom two panels indicate the magnetic scattering due to the transverse spin component.

$T \gtrsim 1.2\,T_N$, the profiles are well described by a single 2D Lorentzian form, that is, $\kappa_\parallel = \kappa_\perp$. As the system is cooled to the immediate vicinity of T_N, the scattering exhibits a crossover from Heisenberg to Ising behavior [14]. Accordingly, we find that within about 20% of T_N, for $T > T_N$, one must describe the lineshape with two components: one 2D Lorentzian with diverging $\xi_\parallel$ and $S_\parallel(0)$, corresponding to the longitudinal ($\parallel$ **c**) Ising fluctuations, and a second 2D Lorentzian corresponding to the non-divergent transverse ($\perp$ **c**) spin fluctuations. For our experimental configuration, the geometrical factors $\sin^2(\phi)$ and $1{+}\cos^2(\phi)$ are both close to unity; specifically, for $E_i = 14.7$ meV, $\sin^2(\phi) \simeq 0.96$ and $1{+}\cos^2(\phi) \simeq 1.04$. The transverse scattering contribution $S_\perp(0)/(1 + q_{2D}^2/\kappa_\perp^2)$ is denoted by the dashed line in the bottom two panels of Figure 2.

In our analysis, we first fit the temperature dependence of the transverse scattering at temperatures below T_N using a very simple model. Within the ordered phase, the transverse spin contribution originates from spin-wave scattering; therefore, $\kappa_\perp$ is held fixed at the spin-wave value of $\kappa_\perp = 0.028$ reciprocal lattice units, while the quantity $S_\perp(0)\kappa_\perp^2$ is assumed to increase with the Bose thermal occupation factor. The Bose factor, which takes into account both neutron energy gain and energy loss due to spin-wave excitations, is $2n(\omega) + 1$ where $n(\omega) = 1/[\exp(\omega/\mathrm{T}) - 1]$ and $\omega = 7.2 \pm 0.2$ K is the low-temperature spin-wave gap at the magnetic zone center [16]. Below T_N we also observe a sharp resolution-limited quasi-2D Bragg component along $(1/2,\ 1/2,\ L)$ which grows in intensity with decreasing temperature. This 2D Bragg scattering probably originates from 2D sheets at the interfaces between the two different 3D stacking domains. The 2D Bragg scattering is assumed to have the same temperature dependence as the 3D order parameter. This simple model is found to describe the data below T_N very well.

Since the focus of our experiments is on the behavior above T_N, the main impetus for measuring and modeling the scattering below T_N is to allow us to estimate the non-critical transverse scattering in the Ising critical regime above T_N. By definition, the transverse scattering must become identical to the longitudinal scattering in

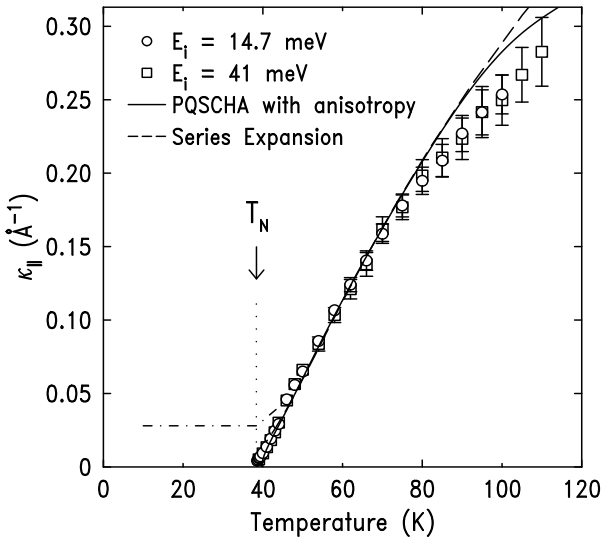

Fig. 3. Temperature dependence of $\kappa_{\|}$, the width of the longitudinal spin component of the critical scattering. At high temperatures, $\kappa_{\|}$ exhibits 2D Heisenberg behavior, crossing over to 2D Ising behavior near T_N. The dash-dotted line represents the interpolated temperature dependence of $\kappa_{\perp}$. The solid line is the PQSCHA result [18] modified to include the effects of the Ising anisotropy, and the dashed line is the prediction from series expansion for the $S = 5/2$ 2DSLQHA [7]. The plotted curves have no adjustable parameters

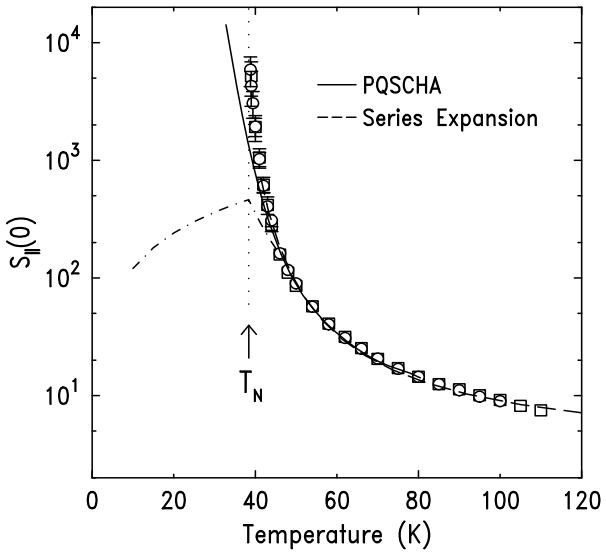

Fig. 4. Temperature dependence of $S_{\|}(0)$, the peak intensity of the longitudinal critical scattering. The dash-dotted line represents the interpolated temperature dependence of $S_{\perp}(0)$. The solid line is the PQSCHA result [18], and the dashed line is the prediction from series expansion for the $S = 5/2$ 2DSLQHA [7]. Since the neutron scattering intensity is not measured in absolute units, the data are scaled to approach optimally the limit $S_{\|}(0) \to S(S+1)/3$ as $T \to \infty$.

the Heisenberg regime well above T_N. Therefore, in the fitting, we assume that for the transverse component, $\kappa_{\perp}$ and $S_{\perp}(0)\kappa_{\perp}^2$ can be simply interpolated linearly between the fitted values at $T_N = 38.4$ K and those at 46 K, and that above 46 K the two Lorentzians are identical, that is, within the errors the system shows pure Heisenberg behavior. Thus, in the final data analysis above T_N, the only free fit parameters are $\kappa_{\|}$ and $S_{\|}(0)$, which describe the Heisenberg behavior at high-temperatures and the Ising critical scattering for temperatures near T_N. The results are shown in Figures 3 and 4. For the fitted values of $\kappa_{\|}$ shown in Figure 3, the plotted error bars correspond to the larger of three statistical standard deviations or one-tenth of the instrumental resolution. Similarly, for the $S_{\|}(0)$ data shown in Figure 4, the plotted error bars are equal to three standard deviations. We note that the data obtained with $E_i = 14.7$ meV and $E_i = 41$ meV agree well with each other, thus confirming the validity of the quasi-elastic approximation [13]. The dash-dotted lines represent the interpolated temperature dependences of the transverse scattering parameters. We find that varying the upper temperature limit of the interpolation of the transverse fluctuations around 46 K by several degrees does not change the results for $\kappa_{\|}$ and $S_{\|}(0)$ within the errors. Furthermore, we also obtain closely similar results using a very different interpolation scheme for $\kappa_{\perp}$ and $S_{\perp}(0)\kappa_{\perp}^2$ similar to that employed in reference [14]. The solid curve in Figure 3 corresponds to a theory for the 2DSLQHA by Cuccoli *et al.* [18], which we plot with a modification incorporating the effects of the Ising anisotropy. We will elaborate upon this in the next Section. The dashed line in Figure 3 is the prediction from high-temperature series expansion for the Heisenberg model with $S = 5/2$ [7]. In Figure 4, the solid line is the unmodified result from reference [18], and the dashed line is the series expansion result for the $S = 5/2$ 2DSLQHA [7]. Since the neutron scattering intensity is not measured in absolute units, we choose a scale for the plot of $S_{\|}(0)$ in Figure 4 such that the data approach optimally the limit $S_{\|}(0) \to S(S+1)/3$ as $T \to \infty$.

Previous studies [14] of the 2D antiferromagnets K_2NiF_4 ($S = 1$) and K_2MnF_4 ($S = 5/2$) show that within $\sim 20\%$ of T_N the critical magnetic scattering follows the behavior predicted for the 2D Ising model, for which the exact exponents are ν=1 for the correlation length and γ=1.75 for the susceptibility. Our main purpose here is to study the 2D Heisenberg regime, so the instrumental resolution was not optimized to investigate the narrow, rapidly diverging peaks in the Ising critical regime. Even so, our fitted values for $\kappa_{\|}$ at temperatures within 20% of T_N yield an exponent of $\nu = 1.0 \pm 0.1$ in good agreement with the exact result $\nu = 1$ for the 2D Ising model.

4 Comparison with theory

A low-temperature theory for the 2DSLQHA was formulated by Chakravarty, Halperin, and Nelson, in which they obtained the static and dynamic properties of the 2DSLQHA by mapping it onto the 2D quantum non-linear σ model [4]. The 2D quantum non-linear σ model is the simplest continuum model which reproduces the

correct spin-wave spectrum and spin-wave interactions of the 2DSLQHA at long wavelengths and low energies [4,19]. First, CHN argued that the 2DSLQHA corresponds to the region of the 2D quantum non-linear σ model in which the ground state is ordered – the renormalized classical regime. Then, CHN used perturbative renormalization group arguments to derive an expression for the correlation length to two-loop order, showing a leading exponential divergence of ξ *versus* inverse temperature. Later, Hasenfratz and Niedermayer employed chiral perturbation theory to calculate the correlation length more precisely to three-loop order [5]. In the renormalized classical scaling regime, the correlation length is given by [5]

$$\frac{\xi}{a} = \frac{e}{8}\frac{c/a}{2\pi\rho_s}\, e^{2\pi\rho_s/T}\left[1 - \frac{1}{2}\left(\frac{T}{2\pi\rho_s}\right) + \mathcal{O}\left(\frac{T}{2\pi\rho_s}\right)^2\right], \tag{4}$$

which we refer to as the CHN-HN formula. The parameters ρ_s and c are the macroscopic spin-stiffness and spin-wave velocity of the model, respectively. For the nearest-neighbor 2DSLQHA, they are related to the microscopic parameters J_{nn}, S and the lattice constant a according to $\rho_s = Z_\rho(S)S^2J_{nn}$ and $c = Z_c(S)2\sqrt{2}aSJ_{nn}$. The coefficients $Z_\rho(S)$ and $Z_c(S)$ are quantum renormalization factors, which can be calculated using spin-wave theory ($S \geq 1/2$), series expansion ($S = 1/2, 1$), and Monte-Carlo techniques ($S = 1/2$) [8,17,20]. For $S = 1/2$, the spin-wave approximation [17] gives $Z_\rho(1/2) \simeq 0.699$ and $Z_c(1/2) \simeq 1.18$, whereas for $S = 5/2$, the factors $Z_\rho(5/2) \simeq 0.951$ and $Z_c(5/2) \simeq 1.03$ are closer to the classical limit of $Z_\rho = Z_c = 1$.

As mentioned above, the correlation length of the $S = 1/2$ system $Sr_2CuO_2Cl_2$ is well described by equation (4) throughout the entire experimental temperature range. Subsequent Monte-Carlo work [8] indicates that this agreement for the $S = 1/2$ case is, at least in part, coincidental; deviations exist, but they are too subtle to be discerned experimentally. In CHN-HN's formulation, the natural expansion parameter for temperature is $T/2\pi\rho_s$. For all experimental systems, the lowest temperature at which 2D Heisenberg behavior can be observed is bounded by a non-zero temperature T_N below which there is 3D long-range order. For the $S = 1/2$ system $Sr_2CuO_2Cl_2$, the measured experimental temperature range is $0.16 < T/2\pi\rho_s < 0.36$ [2]. In our present study of Rb_2MnF_4, which has a higher spin, though smaller J_{nn}, the temperature range is similar, $0.14 < T/2\pi\rho_s < 0.40$. The Monte-Carlo simulations of Beard *et al.* [8] for $S = 1/2$ indicate that the three-loop CHN-HN formula, equation (4), provides an accurate description of the $S = 1/2$ 2DSLQHA for temperatures $T/2\pi\rho_s \lesssim 0.15$. This barely overlaps the temperature range studied experimentally here. Further, for $S = 5/2$ the renormalized classical scaling regime is expected for lower temperatures [7].

In Figure 5, we plot our results for the correlation length *versus* inverse temperature. Since J_{nn} is known from independent experiments [15,16], there are no adjustable parameters in the comparison between theory and

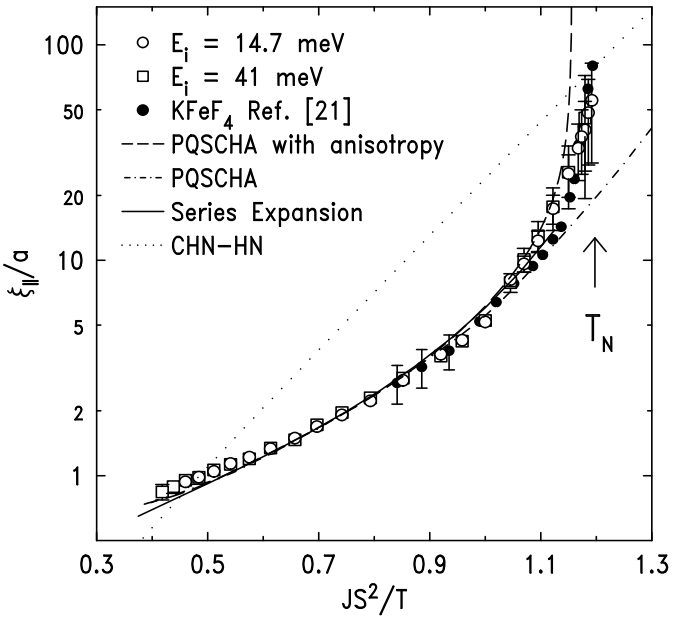

Fig. 5. The longitudinal correlation length $\xi_\parallel = 1/\kappa_\parallel$ *versus* inverse temperature in reduced units. The open symbols are our data for Rb_2MnF_4. The closed circles are results for $KFeF_4$ from reference [21]. The dashed line is the PQSCHA [18] results modified to include the Ising anisotropy. The dash-dotted line is the unmodified PQSCHA result. The solid line is the result of series expansion for the $S = 5/2$ 2DSLQHA [7]. The dotted line is the three-loop CHN-HN formula, equation (4) [4,5]. The comparisons are in absolute units, with no adjustable parameters.

experiment. Also plotted in Figure 5 are the experimental data from Fulton *et al.* [21] for the 2D $S = 5/2$ Heisenberg antiferromagnet $KFeF_4$. The $KFeF_4$ system is less ideal because the nearest neighbor spins in the planes are distorted from a square configuration forming a rectangular lattice. However, using the average of the magnetic exchange coupling along the two different in-plane lattice directions ($J_{nn}^{avg} \simeq 26.9$ K from neutron scattering measurements of the spin-wave dispersion [21] with zero point correction [17]), we find that the agreement for the measured correlation lengths between Rb_2MnF_4 and $KFeF_4$ is excellent. The reduced Ising anisotropy for $KFeF_4$ of $\alpha_I \simeq 0.0045$ is fortuitously almost identical to that for Rb_2MnF_4. The three-loop CHN-HN formula is plotted for $S = 5/2$, and it appears as a straight line on this logarithmic scale. We used the spin-wave theory values of $\rho_s \simeq 5.94J$ and $c \simeq 7.30Ja$ [17]. It is evident that the data deviate significantly from the three-loop CHN-HN result for the quantum non-linear σ model.

Figure 5 also includes the series expansion result for the $S = 5/2$ 2DSLQHA from reference [7]. There is good agreement between the series expansion prediction, with plotted correlation lengths up to 14 lattice constants, and our data over most of the temperature range. Systematic deviations exist at very high temperatures, where the correlation length is small, and at low temperatures near T_N, where the correlation length begins to diverge rapidly.

At high temperatures, where the correlation length decreases to one lattice constant or less, ξ is not precisely defined. Also, at such high temperatures where the measured peaks become broad in reciprocal space, the use of an Ornstein-Zernike Lorentzian lineshape may be called into question, and the background is more difficult to define. Accordingly, it is not surprising that slight deviations exist at high temperatures. We have already pointed out that Ising fluctuations will dominate near T_N, so the correlation length will necessarily deviate from Heisenberg behavior in the immediate vicinity of T_N.

An alternative theoretical analysis of the 2DSLQHA has been carried out by Cuccoli *et al.* [18] in which they treat quantum fluctuations in a self-consistent Gaussian approximation separately from the classical contribution. In their approach, which they label the purely-quantum self-consistent harmonic approximation (PQSCHA), the quantum spin Hamiltonian is rewritten as an effective classical Hamiltonian, where the temperature scale is renormalized due to quantum fluctuations, and the new classical spin length appears as $S + 1/2$. Defining the reduced temperature as $t = T/\{J_{nn}(S + 1/2)^2\}$, the correlation length for the 2DSLQHA is then simply given by

$$\xi(t) = \xi_{cl}(t_{cl}) \quad \text{with} \quad t_{cl} = \frac{t}{\theta^4(t)} \cdot \tag{5}$$

Here, ξ_{cl} is the correlation length for the corresponding classical 2D square-lattice Heisenberg model, and $\theta^4(t)$ is a temperature renormalization parameter. The PQSCHA is most accurate in the limit where the quantum fluctuations are weak, and correspondingly $\theta^4(t)$ is near unity. The calculations of Cuccoli *et al.* [18] show that this is the case for $S = 5/2$ over an extended temperature range; further, their results show good agreement with the existing experimental $S = 1/2$ and $S = 1$ data over the appropriate high-temperature ranges. The behavior of ξ_{cl} is determined from classical Monte-Carlo simulations. The PQSCHA result for $S = 5/2$ is plotted in Figure 5 as the dash-dotted line. Similar to the series expansion result, there is good agreement between the PQSCHA theory and our data and those in $KFeF_4$ with no adjustable parameters. Again, as T_N is approached, the data deviate from the theoretical curve because of the crossover to Ising behavior.

Keimer *et al.* [1] have derived a simple mean-field model which allows one to incorporate the effects on the longitudinal spin correlations of the staggered Ising anisotropy field as appears in equation (1). In this model, the unperturbed Heisenberg correlation length is replaced by the form

$$\xi(\alpha_I, T) = \frac{\xi_{Heis}(T)}{\sqrt{1 - \alpha_I \xi^2_{Heis}(T)}} \cdot \tag{6}$$

Using the value α_I=0.0047 measured in Rb_2MnF_4 and the form for $\xi_{Heis}(T)$ given by the PQSCHA for the Heisenberg model, we obtain the dashed line shown in Figure 5. This mean-field result for the correlation length nicely captures the crossover from Heisenberg to Ising spin correlations in both Rb_2MnF_4 and $KFeF_4$. By design, this model takes into account the growing importance of the local anisotropy field as the spin correlation length grows; it does not include 2D Ising critical effects. Thus, the predicted divergence is mean-field-like with a power-law exponent of ν=1/2 instead of the 2D Ising result of ν=1. This rapid mean-field divergence is also elegantly seen as the "PQSCHA-with-anisotropy" curve rises above our data very close to T_N. Nevertheless, this mean-field model with no adjustable parameters predicts T_N to within 3% in Rb_2MnF_4 and to within 6% in $KFeF_4$. The accuracy of this model is highlighted when compared to the conventional mean-field theory prediction of $T_N = 4J_{nn}S(S + 1)/3$ which is higher than the experimentally measured transition temperatures by more than a factor of two.

In Figure 6 we plot the ratio $S_{\|}(0)/\xi^2_{\|}$ *versus* temperature for Rb_2MnF_4. The open symbols indicate data for which the Ising critical fluctuations become significant, so we concentrate here on the closed symbols in the temperature regime where the behavior is predominantly Heisenberg-like. The low-temperature analysis of CHN-HN predicts that this quantity should follow the form

$$\frac{S(0)}{\xi^2} = A2\pi M_s^2 \left(\frac{T}{2\pi\rho_s}\right)^2 \left[1 + C\frac{T}{2\pi\rho_s} + \mathcal{O}\left(\frac{T}{2\pi\rho_s}\right)^2\right], \tag{7}$$

where M_s is the $T = 0$ staggered magnetization and A and C are universal constants. The same form, which is written above at three-loop order, can also be derived from a renormalization group analysis of the classical model [9,22]. In an alternative approach, Kopietz [24] obtained the leading T^2 behavior based on a Schwinger boson mean-field theory [23]. Using the values for the universal numbers A and C in equation (7) obtained from Monte-Carlo calculations on the $S = 1/2$ and $S = 1$ models ($A = 4.5$ and $C = 0.5$) [25,26], we plot equation (7) in Figure 6. It appears that the low-temperature data points in the Heisenberg regime may overlap with the T^2 law; however, the data depart significantly from the predicted T^2 law at higher temperature. Since the overall scaling factor for the $S_{\|}(0)$ data was determined in Figure 4, there are no adjustable parameters in this plot. Also plotted are results from series expansion [7] and the PQSCHA theory [18] for the $S = 5/2$ 2DSLQHA. There is a rough overall agreement with both of these latter results, but systematic deviations clearly exist.

5 Summary

In summary, we find that the instantaneous spin-spin correlations in Rb_2MnF_4 are quantitatively described by high-temperature series expansion results and the PQSCHA theory for the $S = 5/2$ 2DSLQHA with no adjustable parameters. There is also good absolute agreement with previous results for $KFeF_4$, which is a somewhat less ideal $S = 5/2$ 2DSLQHA. Our data, which

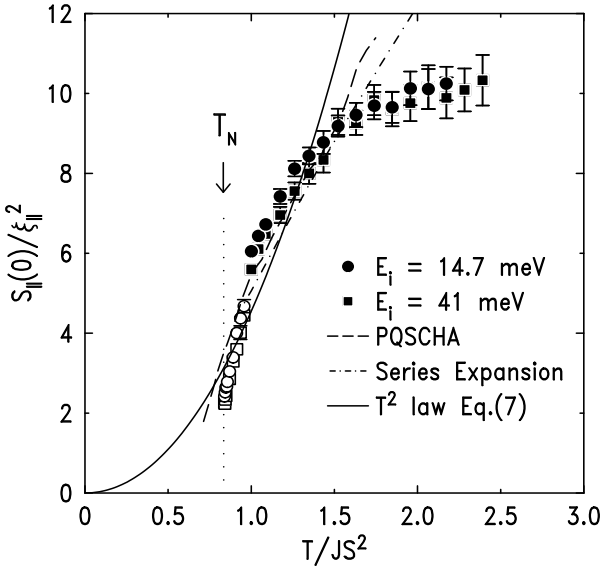

Fig. 6. The ratio $S_{\|}(0)/\xi_{\|}^2$ *versus* temperature. The dashed line is the PQSCHA result [18]. The dash-dotted line is the prediction from series expansion for the $S = 5/2$ 2DSLQHA [7]. The solid line is equation (7) with the parameters A and C obtained from [26].

correspond to correlation lengths up to about 50 lattice constants, are not well described by the three-loop CHN-HN prediction based on the 2D quantum non-linear σ model. This discrepancy almost certainly derives from the fact that the experimental data correspond to temperatures where the $S = 5/2$ 2DSLQHA is not in the renormalized classical low-temperature regime described by equation (4), but rather in the classical scaling regime [9]. Arguments by Elstner *et al.* [7], based on CHN's use of cutoff wavevectors for integrations over the Brillioun zone, give a crossover temperature $T_{cr} \sim J_{nn}S$ between renormalized classical behavior at low-temperature and classical scaling behavior at high-temperature. For Rb_2MnF_4, $T_{cr} \sim 18.4$ K, which suggests that the experimental data lie in the classical scaling regime. In addition, the PQSCHA theory predicts the correlation length accurately in absolute units for this material, which is consistent with the statement that quantum fluctuations are not large and the system is in the classical scaling regime in the temperature range measured.

As of yet, no quantum Monte-Carlo results exist for the $S = 5/2$ 2DSLQHA. In Monte-Carlo work for $S = 1/2$ [8,25] it was found that ξ deviates somewhat from the three-loop CHN-HN result for correlation lengths less than $\sim$ 1000 lattice constants. However, results for the ratio $S(0)/\xi^2$ [25] with fitted universal constants show quantitative agreement with the T^2 law of equation (7) over the complete temperature range. Recent Monte-Carlo work for $S = 1$ [26] shows that for correlation lengths of less than 25 lattice constants, ξ is not well described by the three-loop CHN-HN low-temperature formula. However, the $S = 1$ Monte-Carlo data match well both the results from the PQSCHA theory for $S = 1$ and the experimental data for La_2NiO_4. Also, the leading T^2 behavior for $S(0)/\xi^2$ is followed by the Monte-Carlo data for $S = 1$. This is in contrast with our results for Rb_2MnF_4 where we find a significant departure from the leading T^2 behavior for $S(0)/\xi^2$ at high temperatures or, equivalently, short correlation lengths.

Finally, we note that the 2D Heisenberg-Ising crossover behavior in both Rb_2MnF_4 and $KFeF_4$ is predicted reasonably well by equation (6) without any adjustable parameters. However, since equation (6) is a mean-field result it cannot account for the asymptotic 2D Ising critical behavior.

In conclusion, we now have a quite complete understanding of the spin correlation length in the $S = 5/2$ 2D Heisenberg antiferromagnet for the experimentally relevant temperature range. Further work is required to understand the static structure factor peak intensity $S(0)$ to the same degree.

We thank N. Elstner and R.R.P. Singh for providing us with the series expansion results, and we thank P. Verrucchi for sending us the numerical PQSCHA results. We thank U.-J. Wiese for helpful discussions. The work at MIT was supported by the National Science Foundation – Low Temperature Physics Program under award number DMR 97-04532. Work at Brookhaven National Laboratory was carried out under Contract No. DE-AC02-98CH10886, Division of Materials Science, U.S. Department of Energy.

References

1. B. Keimer, N. Belk, R.J. Birgeneau, A. Cassanho, C.Y. Chen, M. Greven, M.A. Kastner, A. Aharony, Y. Endoh, R.W. Erwin, G. Shirane, Phys. Rev. B **46**, 14034 (1992); R.J. Birgeneau, A. Aharony, N.R. Belk, F.C. Chou, Y. Endoh, M. Greven, S. Hosoya, M.A. Kastner, C.H. Lee, Y.S. Lee, G. Shirane, S. Wakimoto, B.O. Wells, K. Yamada, J. Phys. Chem. Solids **56**, 1913 (1995).
2. M. Greven, R.J. Birgeneau, Y. Endoh, M.A. Kastner, B. Keimer, M. Matsuda, G. Shirane, T.R. Thurston, Phys. Rev. Lett. **72**, 1096 (1994); M. Greven, R.J. Birgeneau, Y. Endoh, M.A. Kastner, M. Matsuda, G. Shirane, Z. Phys. B **96**, 465 (1995).
3. M.S. Makivić H.-Q. Ding, Phys. Rev. B **43**, 3562 (1991).
4. S. Chakravarty, B.I. Halperin, D.R. Nelson, PRB **39**, 2344 (1989); S. Chakravarty, B.I. Halperin, D.R. Nelson, PRL **60**, 1057 (1988).
5. P. Hasenfratz F. Niedermayer, Phys. Lett. B **268**, 231 (1991).
6. K. Nakajima, K. Yamada, S. Hosoya, Y. Endoh, M. Greven, R.J. Birgeneau, Z. Phys. B **96**, 479 (1995).
7. N. Elstner, A. Sokol, R.R.P. Singh, M. Greven, R.J. Birgeneau, Phys. Rev. Lett. **75**, 938 (1995). The series expansion results plotted in the current paper were provided to us by R.R.P. Singh.
8. B.B. Beard, R.J. Birgeneau, M. Greven, U.-J. Wiese, Phys. Rev. Lett. **80**, 1742 (1998).
9. N. Elstner, Int. J. Mod. Phys. B **11**, 1753 (1997). For a discussion of various crossovers such as that between renormalized classical scaling and classical scaling, see A. Sokol, N. Elstner, R.R.P. Singh, unpublished paper (1995), available as cond-mat/9505148.

10. R.J. Birgeneau, H.J. Guggenheim, G. Shirane, Phys. Rev. B **1**, 2211 (1970).
11. R.A. Cowley, A. Aharony, R.J. Birgeneau, R.A. Pelcovits, G. Shirane, T.R. Thurston, Z. Phys. B **93**, 5 (1993).
12. R.J. Birgeneau, H.J. Guggenheim, G. Shirane, Phys. Rev. Lett. **22**, 720 (1969); J. Skalyo, Jr., G. Shirane, R.J. Birgeneau, H.J. Guggenheim, Phys. Rev. Lett. **23**, 1394 (1969); R.J. Birgeneau, H.J. Guggenheim, G. Shirane, Phys. Rev. B **8**, 304 (1973).
13. R.J Birgeneau, J. Skalyo Jr., G. Shirane, Phys. Rev. B **3**, 1736 (1971).
14. R.J. Birgeneau, J. Als-Nielsen, G. Shirane, Phys. Rev. B **16**, 280 (1977).
15. H.W. deWijn, L.R. Walker, R.E. Walstedt, Phys. Rev. B **8**, 285 (1973).
16. R.A. Cowley, G. Shirane, R.J. Birgeneau, H.J. Guggenheim, Phys. Rev. B **15**, 4292 (1977).
17. C.J. Hamer, Z. Weihong, J. Oitmaa, Phys. Rev. B **50**, 6877 (1994); J. Igarashi, Phys. Rev. B **46**, 10763 (1992).
18. A. Cuccoli, V. Tognetti, R. Vaia, P. Verrucchi, Phys. Rev. B **56**, 14456 (1997); A. Cuccoli, V. Tognetti, R. Vaia, P. Verrucchi, Phys. Rev. Lett. **77**, 3439 (1996).
19. E. Manousakis, Rev. Mod. Phys. **63**, 1 (1991).
20. U.-J. Wiese, H.P. Ying, Z. Phys. B **93**, 147 (1994).
21. S. Fulton, R.A. Cowley, A. Desert, T. Mason, J. Phys. Condens. Matter **6**, 6679 (1994); S. Fulton, S.E. Nagler, L.M.N. Needham, B.M. Wanklyn, J. Phys. Condens. Matter **6**, 6667 (1994).
22. D.R. Nelson, R.A. Pelcovits, Phys. Rev. B **16**, 2191 (1977).
23. A. Auerbach, D. Arovas, Phys. Rev. Lett. **61**, 617 (1988).
24. P. Kopietz, Phys. Rev. Lett. **64**, 2587 (1990).
25. J.-K. Kim, M. Troyer, Phys. Rev. Lett. **80**, 2705 (1998).
26. K. Harada, M. Troyer, N. Kawashima, J. Phys. Soc. Jap. **67** (in press, 1998).